

## Chapter 1. Plasma Dynamics

### Academic and Research Staff

Professor Abraham Bers, Professor Bruno Coppi, Dr. Stefano Migliuolo, Dr. Abhay K. Ram, Dr. Linda E. Sugiyama

### Visiting Scientists and Research Affiliates

Dr. Augusta Airoldi, Dr. Giuseppe Bertin, Dr. Francesca Bombarda, Dr. Giovanna Cenacchi, Dr. Vladimir Fuchs,<sup>1</sup> Dr. Riccardo Maggiore, Dr. Francesco Pegoraro, Dr. Marco Riccitelli, Dr. Joachim Theilhaber,<sup>2</sup> Franco Carpignano, George M. Svols

### Graduate Students

Ronak J. Bhatt, Ronald J. Focia, Gregory Penn, Ante Salcedo, Steven D. Schultz, Alexander Seidel

### Undergraduate Students

Leiter Kang

### Technical and Support Staff

Laura M. von Bosau

## 1.1 Plasma Wave Interactions – RF Heating and Current Generation

### 1.1.1 Introduction

As outlined in *RLE Progress Report No. 140*,<sup>3</sup> the theoretical and computational effort of this group is concerned with plasma electrodynamics problems related to heating and current drive in magnetically confined plasmas, light scattering instabilities in laser-plasma interactions of interest to inertial confinement of plasmas, and nonlinear and chaotic multiple wave-particle interaction mechanisms with application to understanding observed ion energization in space plasmas.

Section 1.1.2 reports on the interaction of RF current drive with the bootstrap current in tokamaks—a study of importance to the achievement of efficient steady-state operation in tokamaks. Section 1.1.3 describes progress in understanding nonlinear and chaotic dynamics in the interaction of ions with two non-colinear waves propagating across the magnetic field of a plasma; the detailed report on colinear waves was

given in *RLE Progress Report No. 140*.<sup>3</sup> The third report (1.1.4) is a continuation of our effort in describing the three-dimensional evolution in time of laser-plasma instabilities. The fourth section (1.1.5) reports on our work of interest to the National Spherical Torus Experiment for which we have proposed new means of plasma heating and current drive.<sup>3</sup>

### 1.1.2 Interaction of Bootstrap Current and RF Waves in Tokamaks

#### Sponsor

U.S. Department of Energy  
Grant DE-FG02-91ER-54109

#### Project Staff

Steven D. Schultz, Professor Abraham Bers, Dr. Abhay K. Ram

Work is in progress on the interaction of radio frequency (RF) waves and the bootstrap current in tokamaks. By using a Fokker-Planck collisional/quasilinear code, we have performed a kinetic calcu-

<sup>1</sup> Centre Canadien de Fusion Magnétique (CCFM), Québec, Canada.

<sup>2</sup> Whitehead Institute, MIT Center for Genome Research, Cambridge, Massachusetts.

<sup>3</sup> A. Bers, A.K. Ram, D. Benisti, V. Fuchs, J. Theilhaber, R.J. Focia, A. Salcedo, S.D. Schultz, and K.C. Wu, "Plasma Wave Interactions—RF Heating and Current Generation," *RLE Progress Report No. 140*, (Cambridge: MIT Research Laboratory of Electronics, 1998), pp. 229-48.

lation of the electron current in a prescribed density and temperature gradient, for a toroidally-confined plasma.

The current carried by electrons is found by taking the parallel velocity moment of their distribution function  $f$ ,

$$J_{\parallel} = -e \int d^3v v_{\parallel} f \quad (1)$$

We take  $f$  to be at steady state, averaged over the gyromotion, and independent of the toroidal angle  $\phi$  by axisymmetry. Under these assumptions,  $f$  can be written as a function of the guiding center coordinates  $r$  and  $\theta$  and two constants of the motion, the electron's energy  $E$  and magnetic moment  $\mu$ . Then  $f$  satisfies the drift kinetic equation (DKE)

$$v_{\parallel} \frac{B_{\theta}}{B} \frac{1}{r} \frac{\partial f}{\partial \theta} + v_{Dr} \frac{\partial f}{\partial r} = C(f) + Q(f) \quad (2)$$

where  $C(f)$  is a collision operator, and  $Q(f)$  is the quasilinear operator for diffusion due to RF waves.

In *RLE Progress Report No. 137*,<sup>4</sup> we described one way of solving (2) through expansion in small parameters. The result was

$$f = f_0^{(o)} + \tilde{f}_1^{(o)} + \bar{f}_1^{(o)} \quad (3)$$

The modified electron distribution due to RF effects only was the solution to

$$\left\langle C(f_0^{(o)}) + Q(f_0^{(o)}) \right\rangle = 0 \quad (4)$$

where the brackets indicate averaging over a bounce orbit. Inclusion of guiding center drifts gives

$$\tilde{f}_1^{(o)} = -\frac{m}{eB_{\theta}} v_{\parallel} \frac{\partial f_0^{(o)}}{\partial r}, \quad (5)$$

and the additional equation

$$\left\langle C(\tilde{f}_1^{(o)}) + Q(\tilde{f}_1^{(o)}) \right\rangle = S \quad (6)$$

with the "source term"

$$S \equiv -\left\langle C(\tilde{f}_1^{(o)}) + Q(\tilde{f}_0^{(o)}) \right\rangle \quad (7)$$

We have been able to reproduce the neoclassical distribution with the Fokker-Planck/neoclassical code FASTFP-NC. This code incorporates the Fokker-Planck code FASTFP,<sup>5</sup> which was created by M. Shoucri and I. Shkarofsky, in order to solve the equations (4) and (6). The code contains a collision operator with both electron-electron and electron-Maxwellian ion collisions, and all of the formulation is relativistic. The code solves the equation on multiple flux surfaces, assuming a fixed density and background ion temperature, and also includes the particle drifts due to magnetic field gradient and curvature.

Since FASTFP was designed for RF current drive calculations only, a significant amount of modification was necessary to include bootstrap currents:

- Correct treatment of trapped electrons and the boundary between trapped and passing electrons.
- The flux-surface averaged source term (7) requires a more complex integration due to the  $\theta$  dependence of  $\tilde{f}_1^{(o)}$ .
- Collisions with ions must be treated correctly, including the neoclassical ion parallel flow that contributes to the bootstrap current.
- Improved accuracy was implemented to allow detection of small synergistic differences in the combined RF-bootstrap current.

As an essential first step to verification of the usefulness of FFP-NC, accurate calculations of the bootstrap current without RF waves were performed, and compared to values of the bootstrap current derived by theory.<sup>6</sup> The results are shown in Figure 1 and Figure 2, for parameters typical of Tore Supra and JT-60U, respectively.

4 A. Bers, A.K. Ram, C. Chow, V. Fuchs, K.P. Chan, S.D. Schultz, and L. Vacca, "Plasma Wave Interactions—RF Heating and Current Generation," *RLE Progress Report No. 137* (Cambridge: MIT Research Laboratory of Electronics, 1995), pp. 229-48.

5 M. Shoucri and I. Shkarofsky, "A Fast 2D Fokker-Planck Solver With Synergetic Effects," *Comput. Phys. Commun.* 82: 287 (1994); M. Shoucri, I. Shkarofsky, and Y. Peysson, "Numerical Solution of the Fokker-Planck Equation for the Heating and Current Drive Problem," Centre Canadien de Fusion Magnétique Report No. CCFM-RI-465e (Varennes, Québec, Canada: Institut de Recherche de l'Hydro Québec, 1996); M. Shoucri and I. Shkarofsky, "A Fokker-Planck Code for the Electron-Cyclotron Current Drive and Electron-Cyclotron/Lower Hybrid Current Drive Synergy," *Centre Canadien de Fusion Magnétique Report No. CCFM-RI-467e* (Varennes, Québec, Canada: Institut de Recherche de l'Hydro Québec, 1996).

6 S.P. Hirshman, "Finite-Aspect-Ratio Effects on the Bootstrap Current in Tokamaks," *Phys. Fluids* 31: 3150 (1988).

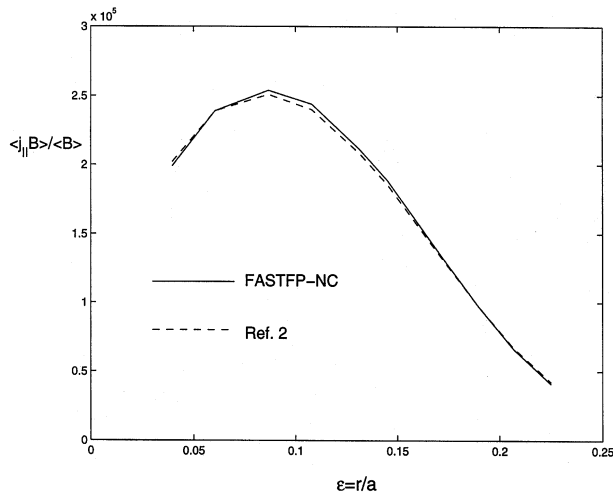


**Figure 1.** Bootstrap current  $J_{\parallel}^{\text{BS}}$  for a Maxwellian plasma from FASTFP-NC (solid line) and Hirshman<sup>7</sup> (dashed line), for Tore Supra parameters:  $R_0 = 2.37$  m,  $a = 0.715$  m,  $n_e = (7 \times 10^{19} \text{ m}^{-3}) \times [1 - (r/a)^2]^{0.8}$ ,  $B_T = 2.15$  T,  $T_e = (3.55 \text{ keV}) \times [1 - (r/a)^2]^{4.8}$ ,  $T_i = (1.55 \text{ keV}) \times [1 - (r/a)^2]^{4.8}$ .

The FASTFP-NC code will be utilized to consider the effect of neoclassical kinetics on several RF current drive scenarios. We divide these into three types:

1. In lower hybrid current drive (LHCD), waves with high parallel phase velocity interact with the electron distribution through Landau damping, which diffuses electrons to increase  $v_{\parallel}$ , pulling out a "tail" of energetic electrons.
2. In fast wave current drive (FWCD), low frequency waves are used which do not damp as strongly as lower hybrid waves and thus can interact with electrons at  $v_{\parallel} = v_t$  and below. This means they often interact with trapped particles, an effect that is undesirable for simple current drive theory. However, we consider that if these waves work to de-trap electrons preferentially in the bootstrap current direction, they might synergistically enhance the overall noninductive current drive of bootstrap current and FWCD.

3. Electron cyclotron (EC) waves, interacting with electrons through cyclotron damping, diffuse electrons to higher values of  $v_{\perp}$  and thus are often used to heat the plasma. The increase of  $v_{\perp}$  moves more electrons into trapped orbits, an effect which can increase the bootstrap current, according to recent theory.<sup>8</sup> In addition, EC waves contribute to current drive if launched with an asymmetry in parallel phase velocity.

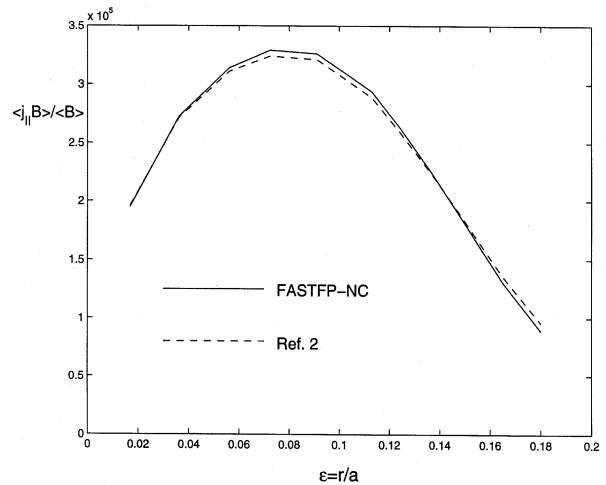


**Figure 2.** Bootstrap current  $J_{\parallel}^{\text{BS}}$  for a Maxwellian plasma from FASTFP-NC (solid line) and Hirshman<sup>8</sup> (dashed line), for JT-60U parameters:  $R_0 = 2.89$  m,  $a = 0.75$  m,  $n_e = (6.1 \times 10^{19} \text{ m}^{-3}) \times [1 - (r/a)^2]^{3.5}$ ,  $B_T = 4.5$  T,  $T_e = (3.55 \text{ keV}) \times [1 - (r/a)^2]^5$ ,  $T_i = (7.7 \text{ keV}) \times [1 - (r/a)^2]^5$ .

The data which was compiled in *Progress Report No. 139*<sup>9</sup> has been corrected as a result of later modifications of the FASTFP-NC code, as discussed above. A few early runs with the corrected code have been produced, and are given in Table 1. The runs were taken with parameters typical of the profiles of the Tore Supra tokamak given in the caption to Figure 1.

7 S.P. Hirshman, "Finite-Aspect-Ratio Effects on the Bootstrap Current in Tokamaks," *Phys. Fluids* 31: 3150 (1988).

8 P. Helander, R.J. Hastie, and J.W. Connor, "The Bootstrap Current in a Tokamak With Electron Cyclotron Heating," *Phys. Plasmas* 4: 3211 (1997).

9 A. Bers, A.K. Ram, D. Benisti, V. Fuchs, J. Theilhaber, R.J. Focia, F.W. Galicia, S.D. Schultz, L. Vacca, and K.C. Wu, "Plasma Wave Interactions—RF Heating and Current Generation," *RLE Progress Report No. 139* (Cambridge: MIT Research Laboratory of Electronics, 1997), pp. 233-47.

**Table 1: Electron current  $J_{||}$  from FASTFP-NC which includes neoclassical effects and an RF parallel diffusion coefficient, separately and together.**

Type	D	$J_{  }$ from FASTFP-NC in MA/m <sup>2</sup>				$\eta=(J_{  }-J_{BS})/P_{abs}$	
		Bootstrap	RF Only	Combined	Synergist.	$J_{BS} = 0$	With NC
LH	0.5	0.27	0.62	0.92	0.03	19.0	26.9
EC	0.05	0.27	0.75	1.05	0.04	3.73	4.13

In each case in Table 1, D is a diffusion coefficient, normalized to units of  $v_c p_t^2$ . In the lower hybrid case, the diffusion is in the parallel momentum direction,

$$Q_{LH}(f) = \frac{\partial}{\partial p_{||}} D \frac{\partial f}{\partial p_{||}} \quad (8)$$

in a range of parallel velocities  $4v_t < v_{||} < 8v_t$ , while in the electron cyclotron case, the diffusion operator has the form

$$Q_{EC}(f) = \left( \frac{\partial}{\partial E} + \frac{N_{||}}{c} \frac{\partial}{\partial p_{||}} \right) D \left( \frac{\partial}{\partial E} + \frac{N_{||}}{c} \frac{\partial}{\partial p_{||}} \right) f \quad (9)$$

on the resonance curve  $\gamma - N_{||} v_{||} / c = 0.94$ , with  $N_{||} = 0.5$ . The current drive efficiency  $h$ , which is normalized to  $e/v m v_t$ , is calculated by taking the total non-inductive current and subtracting the bootstrap current in the absence of RF waves, then dividing by the RF power absorbed by the plasma.

With the FASTFP-NC code giving good results, we will continue to explore different RF scenarios. In addition, the results should continue to aid in the development of theory for the synergistic effects. Early results show an improved coupling of RF for current drive in the tail, far from the trapped region of phase space, due to the perturbing effect of the radial drift motion of electrons. The adjoint technique using the Spitzer-Härm distribution will be used to verify this effect. The effect of diffusion into and out of the trapped electron region in Fast-Wave and Electron-

Cyclotron RF scenarios will be further tested to see if greater effects are observed. Strong EC heating will be studied to observe the predicted increase in the bootstrap current, and combinations of waves, such as an EC heating and LH current drive, will also be considered.

### 1.1.3 Energization of Ions by Two Lower Hybrid Waves

#### Sponsor

National Science Foundation  
Grant ATM 98-06328

#### Project Staff

Dr. Abhay K. Ram, Leiter Kang, Professor Abraham Bers

In *RLE Progress Report No. 140*,<sup>10</sup> we described a theoretical model for understanding observed energization of ionospheric oxygen ions by lower hybrid waves. This model was based on a new phenomenon of nonlinear coherent energization by multiple electrostatic waves that has been previously discussed.<sup>10</sup> The details of the nonlinear coherent energization process and the energization to high energies by electrostatic waves have been the subject of some of our recent publications.<sup>11</sup> We had also developed a possible scenario that takes advantage of this nonlinear coherent energization process for ion heating by lower hybrid waves in laboratory tokamak plasmas.<sup>12</sup> In this case, our studies were based

10 A. Bers, A.K. Ram, D. Benisti, V. Fuchs, J. Theilhaber, R.J. Focia, A. Salcedo, S.D. Schultz, and K.C. Wu, "Plasma Wave Interactions—RF Heating and Current Generation," *RLE Progress Report No. 140* (Cambridge: MIT Research Laboratory of Electronics, 1998), pp. 229-48.

11 D. Benisti, A.K. Ram, and A. Bers, "Ion Dynamics in Multiple Electrostatic Waves in a Magnetized Plasma - Part I: Coherent Acceleration," *Phys. Plasmas* 5: 3224 (1998); D. Benisti, A.K. Ram, and A. Bers, "Ion Dynamics in Multiple Electrostatic Waves in a Magnetized Plasma - Part II: Enhancement of the Acceleration," *Phys. Plasmas* 5: 3233 (1998); A.K. Ram, A. Bers, and D. Benisti, "Ionospheric Ion Acceleration by Multiple Electrostatic Waves," *J. Geophys. Res.* 103: 9431 (1998).

12 A. Bers, A.K. Ram, D. Benisti, V. Fuchs, J. Theilhaber, R.J. Focia, A. Salcedo, S.D. Schultz, and K.C. Wu, "Plasma Wave Interactions—RF Heating and Current Generation," *RLE Progress Report 140* (Cambridge, Massachusetts: Research Laboratory of Electronics, 1998) pp. 229-48.

on two lower hybrid waves that are colinear and propagating across the ambient magnetic field. We have generalized this to the case of two lower hybrid waves that are not colinear. We find that the process of nonlinear coherent energization occurs if the angle between the two waves is less than a critical angle. Below we give the results from this analysis.

The motion of an ion interacting with two plane electrostatic waves, propagating perpendicularly to an ambient uniform magnetic field,  $\vec{B} = B_0 \hat{z}$ , is given by

$$\frac{dx}{dt} = v_x \quad (10)$$

$$\frac{dy}{dt} = v_y \quad (11)$$

$$\frac{dv_x}{dt} = \Omega v_y + \frac{QE_1}{M} \sin(k_1 x - \omega_1 t) + \frac{QE_2}{M} \cos(\phi) \sin[k_2 \cos(\phi) x + k_2 \sin(\phi) y - \omega_2 t + \zeta] \quad (12)$$

$$\frac{dv_y}{dt} = -\Omega v_x + \frac{QE_2}{M} \sin(\phi) \sin \left[ \begin{array}{l} k_2 \cos(\phi) x + \\ k_2 \sin(\phi) y - \omega_2 t + \zeta \end{array} \right] \quad (13)$$

where  $v_x$  and  $v_y$  are the x and y components, respectively, of the velocity of an ion of charge Q and mass M,  $E_i$  is the electric field amplitude of the ith plane wave with wavenumber  $k_i$  and angular frequency  $\omega_i$ ,  $\Omega = QB_0 / M$  is the ion cyclotron frequency, and  $\zeta$  is an arbitrary fixed phase. Here we have assumed, without loss of generality, that the first wave is propagating along the x-direction and that the angle between the directions of propagation of the two waves is  $\phi$ . If we use the following normalizations:  $\Omega t \rightarrow \tau$ ,  $k_1 x \rightarrow x$ ,  $k_1 y \rightarrow y$ ,  $k_1 v_x / \Omega \rightarrow v_x$ ,  $k_1 v_y / \Omega \rightarrow v_y$ ,  $k_2 / k_1 \rightarrow \kappa$ ,  $\omega_i / \Omega \rightarrow v_i$ , and  $QE_i k_1 / (M\Omega^2) \rightarrow \varepsilon_i$ , the above equations of motion become:

$$\frac{dx}{d\tau} = v_x \quad (14)$$

$$\frac{dy}{d\tau} = v_y \quad (15)$$

$$\frac{dv_x}{d\tau} = v_y + \varepsilon_1 \sin(x - v_1 \tau) + \varepsilon_2 \cos(\phi) \sin[\kappa \cos(\phi) x + \kappa \sin(\phi) y - v_2 \tau + \zeta] \quad (16)$$

$$\frac{dv_y}{d\tau} = -v_x + \varepsilon_2 \sin(\phi) \sin[\kappa \cos(\phi) x + \kappa \sin(\phi) y - v_2 \tau + \zeta] \quad (17)$$

As discussed in *Progress Report No. 140*,<sup>12</sup> for ions whose energies are below the lower energy bound of the chaotic region, we expect that their dynamics can be determined analytically. Toward that end, we carry out a perturbation analysis of (14)-(17) using the method of multiple time scales.<sup>13</sup> The perturbation parameter, in the method of multiple time scales, is the normalized amplitude of the waves. In our analysis, we assume that neither  $v_1$  nor  $v_2$  is an integer, i.e., the wave frequencies are not an integer multiple of the ion-cyclotron frequency. However, we will assume that the difference in the frequencies of the two waves is an integer multiple of the ion-cyclotron frequency, i.e.,  $v_1 - v_2 = N$ , an integer. (The analysis can be generalized to the case when  $v_1 + v_2 = N$ , and also for when  $v_1$  and  $v_2$  are integers.) Our analysis breaks down in the vicinity of the chaotic regime. Upon carrying the multiple time scale analysis to second order in the amplitudes, we find that an approximate solution of (14)-(17) is given by:

$$x(\tau) \approx \rho(\tau) \sin[\tau + \varphi(\tau)] \quad (18)$$

where the evolution of  $\rho$  and  $\varphi$  is determined from the Hamiltonian:

$$H(I, \varphi, \tau) = S_1(I) + S_2(I) \cos(N\varphi - \zeta) + S_3(I) \sin(N\varphi - \zeta) \quad (19)$$

Here  $I = \rho^2/2$  and  $\varphi$  are the canonical coordinates, and the functions  $S_1$ ,  $S_2$ , and  $S_3$  are given by:

$$S_1(I) = \frac{1}{4} \sum_{\ell=-\infty}^{\infty} \frac{\varepsilon_1^2 J_\ell^2(\sqrt{2I}) + \varepsilon_2^2 \cos(2\phi) J_{\ell-N}^2(\kappa\sqrt{2I})}{1 - (\ell - v_1)^2} \quad (20)$$

13 A.H. Nayfeh, *Perturbation Methods* (New York: John Wiley, 1973), pp. 228-307.

$$S_2(l) = \frac{\epsilon_1 \epsilon_2}{2} \sum_{\ell=-\infty}^{\infty} \frac{J_{\ell}(\sqrt{2l}) J_{\ell-N}(\kappa\sqrt{2l})}{1 - (\ell - v_1)^2} \times \left\{ \cos(\phi) \cos[(N - \ell)\phi] - \frac{\sin(\phi) \sin[(N - \ell)\phi]}{\ell - v_1} \right\} \quad (21)$$

$$S_3(l) = \frac{\epsilon_1 \epsilon_2}{2} \sum_{\ell=-\infty}^{\infty} \frac{J_{\ell}(\sqrt{2l}) J_{\ell-N}(\kappa\sqrt{2l})}{1 - (\ell - v_1)^2} \times \left\{ \cos(\phi) \sin[(N - \ell)\phi] + \frac{\sin(\phi) \cos[(N - \ell)\phi]}{\ell - v_1} \right\} \quad (22)$$

It is interesting to note that if we set  $\phi = 0$ , i.e., the two waves are colinear, and  $\zeta = 0$ , then  $S_3(l) = 0$ , and we get the same result discussed in *Progress Report No. 140*.<sup>14</sup> It is easy to note that  $H_- \leq H \leq H_+$  where

$$H_{\pm} = S_1 \pm \sqrt{S_2^2 + S_3^2} \quad (23)$$

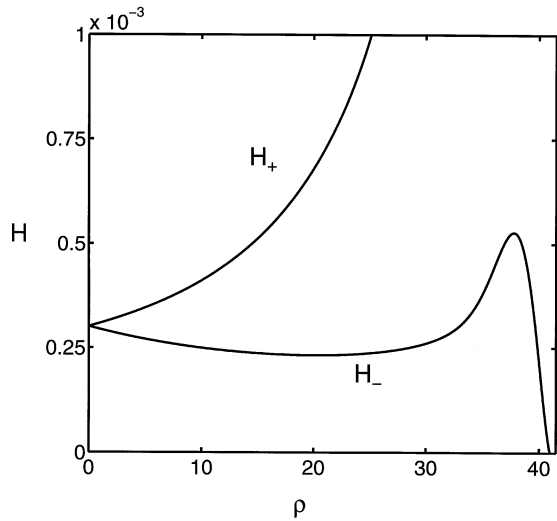


**Figure 3.**  $H_+$  and  $H_-$  versus  $\rho$  for  $v_1 = 40.3$ ,  $v_2 = 41.3$ ,  $\kappa = 1.0$ ,  $\epsilon = \epsilon_2/\epsilon_1 = 1.0$ ,  $\phi = 0$ .

In Figure 3 and Figure 4, we have plotted the curves of  $H_+$  and  $H_-$  for two different  $\kappa$ 's and  $\phi$ 's. It is evident that in both cases, ions from low energy regions (corresponding to low  $\rho$ 's) can be energized into the chaotic regions. (These parameters are similar to the ones used in Figures 8-11 in *Progress Report No.*

140,<sup>14</sup> and the interpretation of Figure 3 and Figure 4 plotted here is similar to that of last year's report.) Thus, nonlinear coherent energization persists even when the two waves are not colinear.

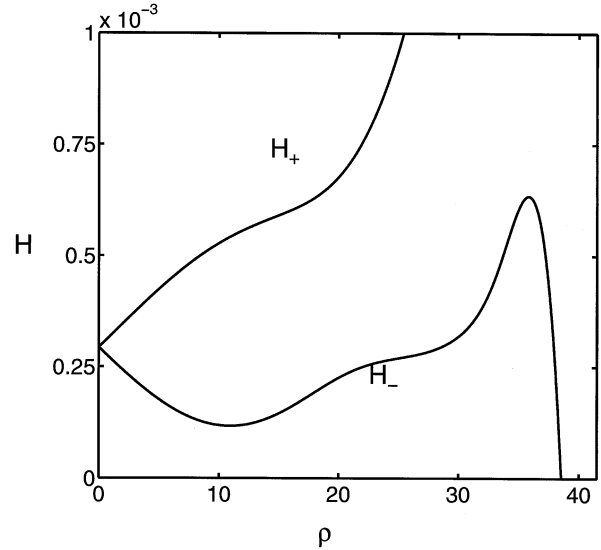


**Figure 4.**  $H_+$  and  $H_-$  versus  $\rho$  for the same parameters as in Figure 3 except that  $\kappa = 1.03$  and  $\phi = 0.05\pi$ .

#### 1.1.4 Relativistic and Phenomenological Mode Damping Effects on the Space-Time Evolution of Laser-Plasma Instabilities

##### Sponsors

Los Alamos National Laboratory

Grant E29060017-8F

U.S. Department of Energy

Grant DE-FG02-91ER-54109

##### Project Staff

Ronald J. Focia, Professor Abraham Bers, Dr. Abhay K. Ram

The work outlined in this report further investigates research presented in *Progress Report No. 140*.<sup>14</sup> In particular, the effects of phenomenological mode damping and relativistic observer velocities on the pulse shape of laser-plasma instabilities relevant to inertial confinement fusion (ICF) are considered.

14 A. Bers, A.K. Ram, D. Benisti, V. Fuchs, J. Theilhaber, R.J. Focia, A. Salcedo, S.D. Schultz, and K.C. Wu, "Plasma Wave Interactions—RF Heating and Current Generation," *RLE Progress Report No. 140* (Cambridge: MIT Research Laboratory of Electronics, 1998), pp. 229-48.

## Time Asymptotic Pulse Shape

The pulse shape of a particular instability is determined by taking the inverse Fourier-Laplace transform of the inverse of the dispersion relation  $D(\omega, \mathbf{k})$  describing the particular three wave interaction. This is known as the Green's function or impulse response and is given by

$$G(\vec{r}, t) = \int_L \frac{d\omega}{2\pi} \int_F \frac{d^3k}{(2\pi)^3} \frac{e^{-i\omega t + i\mathbf{k} \cdot \vec{r}}}{D(\omega, \mathbf{k})} \quad (24)$$

Here, we consider only the logarithmic amplitude of the time asymptotic Green's function given by

$$\ln |G(\vec{r}, t \rightarrow \infty)| = \gamma_p(\vec{V})t \quad (25)$$

which is dominated by the pinch point growthrate  $\gamma_p(\vec{V})$ . The result of the instability analysis in *Progress Report No. 140*<sup>15</sup> yielded the expression for the pinch point growthrate as a function of the parallel component of the observer velocity and is given by

$$\gamma_p(V_{\parallel}) = \frac{2\gamma}{V_1 + V_2} \sqrt{(V_1 - V_{\parallel})(V_{\parallel} + V_2)} \frac{[v_1(V_{\parallel} + V_2) + v_2(V_1 - V_{\parallel})]}{V_1 + V_2} \quad (26)$$

where  $\gamma$  is the coupling constant, and  $v_1$  and  $v_2$  are the daughter wave mode dampings. The definitions and constructions of  $V_{\parallel}$ ,  $V_1$ , and  $V_2$  are repeated in Figure 5 for convenience. In *RLE Progress Report No. 140*,<sup>15</sup> the mode dampings were neglected and relativistic observer velocities were not considered. Here, we extend the instability analysis to include both of these effects.

## Effects of Mode Damping and Relativistic Observer Velocities on the Pulse Shape

As seen in Eq. 26, the effects of mode damping will act to reduce the pinch point growthrate. Inclusion of mode damping can significantly alter the spatial response of the pulse shape, change the instability from being absolute to convective, and in some cases completely quench the instability.

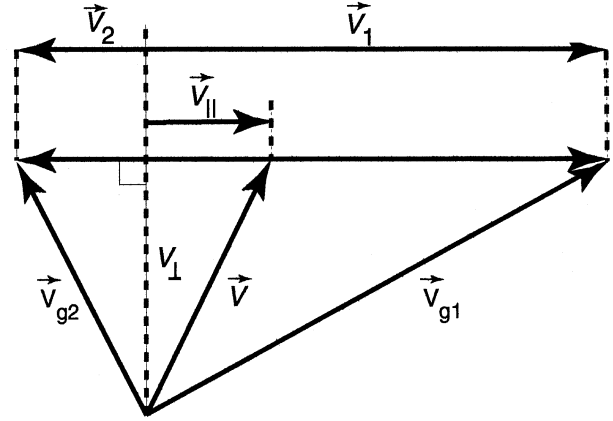


**Figure 5.** Definitions and constructions of velocity vectors in 3-D Green's function evaluation.

In *Progress Report No. 140*,<sup>15</sup> we considered instabilities generated by the interaction of an incident laser pump with a homogeneous plasma. These instabilities have daughter waves consisting of combinations of electromagnetic (EM), electron plasma (EP), and ion acoustic (IA) waves. Electromagnetic waves are damped primarily by electron-ion collisions. The expression for the damping frequency of an EM wave is given by

$$\nu_{ei} = -\frac{2 \cdot 10^{-6} Z n_e \ln(\Lambda)}{T_e^{\frac{3}{2}}}, \quad (27)$$

where  $Z$  is the ion charge,  $n_e$  is the electron density in  $\text{cm}^{-3}$ ,  $\Lambda$  is the plasma parameter and  $T_e$  is the electron temperature in eV. For plasma parameters typical of ICF experiments  $\nu_{ei}$  is several orders of magnitude less than the pinch point growthrate. Mode damping of the EP and IA waves is found by performing a kinetic analysis that involves solution of the plasma dispersion function. The solution for EP waves was performed some time ago.<sup>16</sup> Rather than solving the computationally intensive exact problem, the imaginary part of the electron plasma and ion acoustic dispersion relations were obtained from analytic expressions.<sup>17</sup> These expressions are accurate over a wide range of  $k\lambda_{De}$  (wavevector  $\times$  Debye length) and are provided here for easy reference. The EP mode damping frequency, normalized to the electron plasma frequency, is given by

15 A. Bers, A.K. Ram, D. Benisti, V. Fuchs, J. Theilhaber, R.J. Focia, A. Salcedo, S.D. Schultz, and K.C. Wu, "Plasma Wave Interactions—RF Heating and Current Generation," *RLE Progress Report 140* (Cambridge: MIT Research Laboratory of Electronics, 1998), pp. 229-48.

16 M.A. Lieberman, "Dispersion Diagrams for Hot Electron Plasmas," *RLE Quarterly Progress Report 77* (Cambridge: MIT Research Laboratory of Electronics, 1965), p. 141.

$$v_{EP} = -\sqrt{\frac{\pi}{8}} \frac{1}{K^3} e^{-\frac{3}{2} \frac{1}{2K^2}} \left[ 1 + \left( -0.5K^{0.2} + 9K^{\frac{13}{3}} \right) \left( 1 - e^{-(4.78K)^5} \right) \right], \quad (28)$$

where  $K = k\lambda_{De}$ .

The relativistic correction to the pinch point growth-rate has been derived.<sup>18</sup> The result of this analysis is the relativistic pinch point growthrate given by

$$\gamma_{pR}(V_{\parallel}) = \gamma_p(V_{\parallel}) \sqrt{1 - \left( \frac{V_{\parallel}}{c} \right)^2}. \quad (29)$$

Note that the effects of relativistic observer velocities will only become important when the group velocity of one of the modes present approaches the speed of light. The pinch point growthrate is non-zero only at observer velocities between the extremes of the two mode group velocities (Figure 5). Thus the correction will only be significant for the electromagnetic interactions including stimulated raman scattering (SRS) and stimulated Brillouin scattering (SBS) when the plasma is very underdense.

As an example of neglect and inclusion of the effects discussed in this paper, contour plots of the SRS pulse shape in the x-y plane for a laser propagating in the x-direction and polarized in the z-direction are shown in Figure 6. In Figure 6a without damping the scattered light is predominantly in the backscattered direction. When damping effects are included, Figure 6b shows the maximum pinch point growthrate is reduced and the maximum scattering is now in the side scattered direction. The maximum observer velocity is  $\sim 0.8c$ , and the relativistic correction at this observer velocity is significant ( $\sim 0.6$ ).

An understanding of where the incident laser light is being scattered for a particular interaction is important in laser-plasma experiments. We can qualitatively describe the effects on the pulse shape if, for example, the density is reduced or the laser wavelength is reduced.

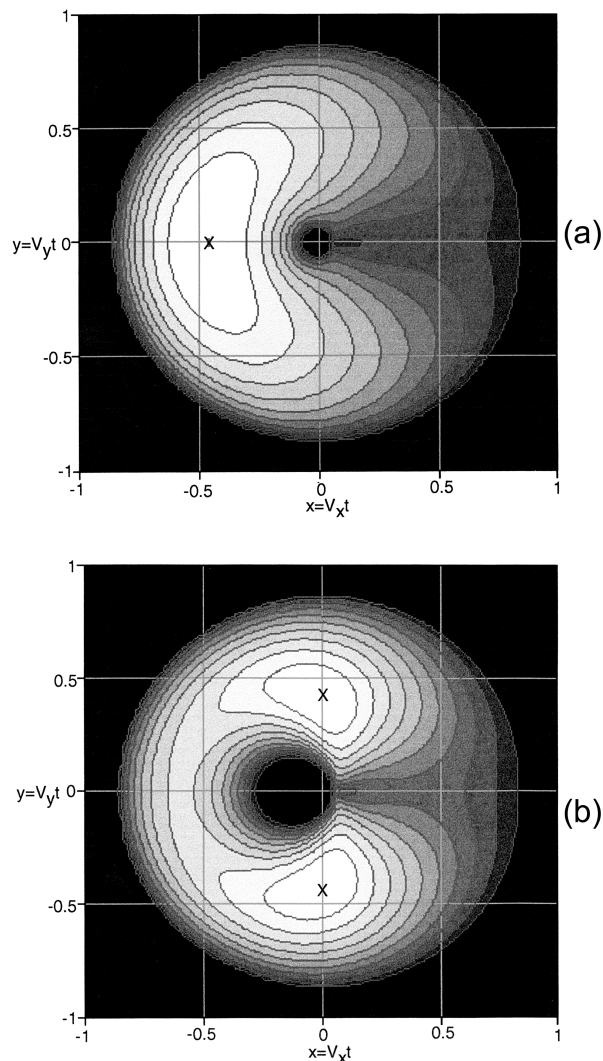


**Figure 6.** Stimulated raman scattering (SRS) pulse shape in the x-y plane for a laser propagating in the x-direction and polarized in the z-direction and parameters  $P_L = 10^{16}$  W/cm<sup>2</sup>,  $\lambda_L = 526.5$  nm,  $T_e = 3$  keV,  $T_i = 500$  eV,  $n_e/n_{crit} = 0.1$ . (a) Mode damping and the relativistic correction are neglected,  $\gamma_{pRmax} = 0.011$ . (b) Mode damping and the relativistic correction are included,  $\gamma_{pRmax} = 0.0073$ ,  $v_{1max} = 1.64 \times 10^{-5}$ ,  $v_{2max} = 1.34 \times 10^{-2}$ , where mode 1 is the electromagnetic wave and mode 2 is the electron plasma wave. The outermost contour is zero, the maximum is marked with an "X," and each contour represents a 10% change.

17 D. Besnard, G. Bonnaud, and G. Schurtz, "Amortissement des Ondes," in *La Fusion Thermonucléaire Intertielle par Laser*, Part 3, R. Dautray and J.-P. Wateau, eds. (Paris, France: Eyrolles, 1993), Chapter 13, pp. 1105-14.

18 A. Bers, A.K. Ram and G. Francis, "Relativistic Analysis of Absolute and Convective Instability Evolutions in Three Dimensions," *Phys. Rev. Lett.* 53: 1457 (1984).

### 1.1.5 Coupling to Electron Bernstein Waves in High- $\beta$ Plasmas

#### Sponsors

Princeton Plasma Physics Laboratory/National  
Spherical Torus Experiment  
Grant S-04020-G PPPL  
U.S. Department of Energy  
Grant DE-FG02-91ER-54109

#### Project Staff

Steven D. Schultz, Professor Abraham Bers, Dr.  
Abhay K. Ram

In *RLE Progress Report No. 140*,<sup>19</sup> we presented our analyses and computations regarding the excitation of electron Bernstein waves (EBW) in NSTX by mode-conversion from an outboard incident extraordinary (X) mode, which can be excited in free space from waveguides just outside the plasma. Another possibility of practical interest entails the excitation (also from waveguides outside the plasma) of an ordinary (O) mode to be incident onto the plasma. The possibility of exciting EBW from an incident O-mode has received considerable attention in the past.<sup>20</sup> This entails two processes of wave transformation: (1) coupling of the O-mode to the slow-extraordinary (SX) mode; followed by (2) mode conversion of the SX-mode to EBW. The first coupling can ideally occur with total power transfer, provided the incident O-mode has a parallel index squared given by

$$n_z^2 = \frac{(\omega_{ce} / \omega)}{1 + (\omega_{ce} / \omega)} \equiv (n_z^2)_{\text{opt}} \quad (30)$$

where  $\omega_{ce}$  is the electron cyclotron frequency and  $\omega$  is the excitation frequency. At this optimum parallel index, the cutoffs of the O-mode and the SX-mode coincide in space so that the incident O-mode energy flow transforms smoothly to energy flow onto the SX-mode. This is corroborated by a full-wave analysis in the quoted references.

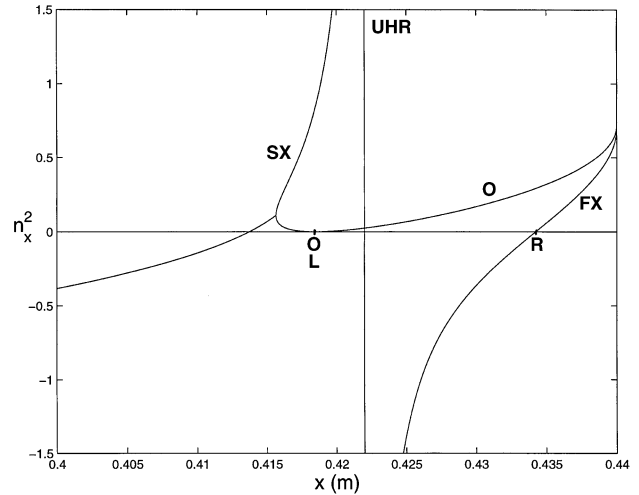


**Figure 7.** Dispersion relation  $n_x^2(x)$  near the outboard edge of NSTX (for plasma parameters and magnetic field profiles, see *Progress Report No. 140*<sup>19</sup>).  $f = 28$  GHz and  $n_z = (n_z)_{\text{opt}} = 0.48$ .

Figure 7 shows the local, cold-plasma dispersion relation of the perpendicular index squared as a function of space near the outboard plasma edge of NSTX (see *Progress Report No. 140*<sup>19</sup> for plasma and magnetic field profile parameters), for  $n_z = n_{z,\text{opt}}$  at a frequency  $f = (\omega/2\pi) = 28$  GHz. Note that the O-mode cutoff position O and the SX-mode cutoff position L coincide. (Contrast this with Figure 2 in *Progress Report No. 140*.<sup>19</sup>) The second process of wave transformation from the SX-mode to EBW has not received a full-wave treatment in the past. Instead, under the assumption that the free space wavelength is much shorter than the density gradient scale length, geometrical optics applied to the propagation of the SX-mode toward the upper-hybrid resonance (UH) layer (modified by finite temperature effects, not shown in Figure 7; see Figure 2 in *RLE Progress Report No. 140*.<sup>19</sup>) totally transforms its energy flow onto an EBW propagating into the plasma.

More generally, and in particular for NSTX, the conditions for the applicability of geometrical optics in coupling SX to EBW are not satisfied and a full wave analysis must be used, as we now show. In particu-

<sup>19</sup> A. Bers, A.K. Ram, D. Benisti, V. Fuchs, J. Theilhaber, R.J. Focia, A. Salcedo, S.D. Schultz, and K.C. Wu, "Plasma Wave Interactions—RF Heating and Current Generation," *RLE Progress Report 140* (Cambridge: MIT Research Laboratory of Electronics, 1998), pp. 229–48.

<sup>20</sup> J. Preinhaelter and V.J. Kopecky, "Penetration of High-Frequency Waves Into a Weakly Inhomogeneous Magnetized Plasma at Oblique Incidence and Their Transformation to Bernstein Modes," *J. Plasma Phys.* 10: 1 (1973); H. Weitzner and D.B. Batchelor, "Conversion Between Cold Plasma Modes in an Inhomogeneous Plasma," *Phys. Fluids* 22: 1355 (1979); E. Mjølhus, "Coupling to Z Mode Near Critical Angle," *J. Plasma Phys.* 31: 7 (1984).

lar, as the SX-mode propagates back toward the UH layer, it can couple back to the fast-extraordinary (FX) mode; thus, part of the incident O-mode can appear as a reflection on the FX-mode and this reduces the mode-conversion from O to EBW. This indeed happens for NSTX at certain frequencies, as shown below. Using our full-wave kinetic code described in *Progress Report No. 140*,<sup>19</sup> we have carried out calculations on possible O to EBW mode conversions for NSTX. Figure 8 (for NSTX plasma parameters<sup>19</sup>) shows the power mode converted to EBW,  $C$ , per unit power in an incident O-mode, as a function of parallel index  $n_z$ , for three different frequencies. The maxima in  $C$  occur exactly at the  $n_z = (n_z)_{\text{opt}}$  where the O and L cutoffs coincide in space. In each case, we find that  $(1 - C_{\text{max}})$  is also precisely the amount of power that appeared as reflected on the FX-mode. This can be understood as follows. The transmission from SX to FX is the same as the transmission from FX to SX, which we calculated in the past:<sup>19</sup>

$$T = e^{-\pi\eta}; \eta \approx \left( \frac{\omega_{\text{ce}}}{\sqrt{2}c} L_n \right)_{\text{UH}} \quad (31)$$

where  $L_n$ , the density gradient scale length, and  $\omega_{\text{ce}}$  are evaluated at the UH layer. Thus, to minimize the transmission from SX to FX requires that  $\eta$  be large, i.e.,  $(L_n)_{\text{UH}}$  large at constant  $(\omega_{\text{ce}})_{\text{UH}}$ . As is clear from the profiles of the various critical frequencies (see Figure 1 in *Progress Report No. 140*<sup>19</sup>),  $(L_n)_{\text{UH}}$  increases with increasing frequency; this reduces  $T$ , and thus the coupling to (i.e., reflection onto) the FX-mode, and hence increases  $C_{\text{max}}$ . Note that in general, mode conversion power to EBW is given by

$$C = 1 - R_O - R_{\text{FX}} \quad (32)$$

where  $R_O$  is the amount of power reflected on the O-mode and  $R_{\text{FX}}$  is the amount of power reflected on the FX-mode. At  $n_z = (n_z)_{\text{opt}}$ ,  $R_O = 0$  and  $(C - 1) = R_{\text{FX}}$  is the amount of power (per unit incident power on the O-mode) coming out as reflected on the FX-mode. As  $n_z$  deviates from  $(n_z)_{\text{opt}}$ , the O and L cutoffs separate and  $R_O$  becomes nonzero.<sup>21</sup> As the frequency increases, the O and L cutoffs move further

into the plasma and separate more rapidly as  $n_z$  deviates from  $(n_z)_{\text{opt}}$ , hence the more rapid decrease in  $C$  with  $n_z \neq (n_z)_{\text{opt}}$ , as shown in Figure 8.

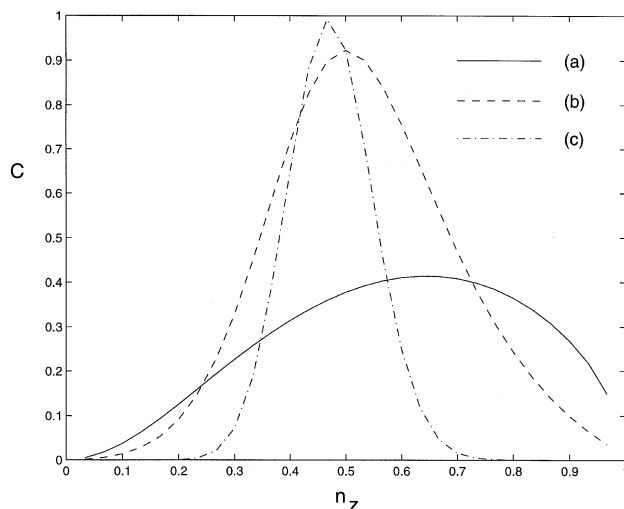


**Figure 8.** Mode conversion to EBW from incident O-mode, in NSTX, as a function of  $n_z$ , for: (a)  $f = 14$  GHz; (b)  $f = 21$  GHz; and (c)  $f = 28$  GHz.

### 1.1.6 Publications

#### Journal Articles

- Bénisti, D., A.K. Ram, and A. Bers. "Ion Dynamics in Multiple Electrostatic Waves in a Magnetized Plasma - Part I: Coherent Acceleration." *Phys. Plasmas* 5: 3224 (1998).
- Bénisti, D., A.K. Ram, and A. Bers. "Ion Dynamics in Multiple Electrostatic Waves in a Magnetized Plasma - Part II: Enhancement of the Acceleration." *Phys. Plasmas* 5: 3233 (1998).
- Bers, A., A.K. Ram, and S.D. Schultz. "Excitation of EBW's in Triplet Mode Conversion Resonator for Heating and Current Drive in NSTX." *Bull. Am. Phys. Soc.* 43: 1863 (1998).
- Focia, R.J., A. Bers, and A. K. Ram. "Stability Analysis of Laser Plasma Interactions Relevant to Inertial Confinement Fusion (ICF)." *Bull. Am. Phys. Soc.* 43: 1794 (1998).
- Ram, A.K., A. Bers, and D. Bénisti. "Ionospheric Ion Acceleration by Multiple Electrostatic Waves." *J. Geophys. Res.* 103: 9431 (1998).

21 J. Preinhaelter and V.J. Kopecky, "Penetration of High-Frequency Waves Into a Weakly Inhomogeneous Magnetized Plasma at Oblique Incidence and Their Transformation to Bernstein Modes," *J. Plasma Phys.* 10: 1 (1973); H. Weitzner and D.B. Batchelor, "Conversion Between Cold Plasma Modes in an Inhomogeneous Plasma," *Phys. Fluids* 22: 1355 (1979); E. Mjølhus, "Coupling to Z Mode Near Critical Angle," *J. Plasma Phys.* 31: 7 (1984).

- Salcedo, A., A.K. Ram, and A. Bers. "Variation of SRS Backscattering Due to Ion Acoustic Wave Damping." *Bull. Am. Phys. Soc.* 43: 1796 (1998).
- Schultz, S.D., A. Bers, and A.K. Ram. "Effects of RF Waves on the Bootstrap Current in Tokamaks." *Bull. Am. Phys. Soc.* 43: 1873 (1998).

### Meeting Papers

- Bers, A., A.K. Ram, and S.D. Schultz. "Coupling to Electron Bernstein Waves in Tokamaks." *Proceedings of the Second Europhysics Topical Conference on RF Heating and Current Drive of Fusion Devices*, Brussels, Belgium, January 20-23, 1998. J. Jacquinot, G. Van Oost, and R.R. Weynants, eds. Petit-Lancy, Switzerland: Contributed Papers, European Physical Society, vol. 22A, 1998, pp. 237-40.
- Ram, A.K. "Acceleration of Ionospheric Ions by Wave-Particle Interactions." Invited paper presented at the 1998 Cambridge Symposium Workshop on the Physics of Space Plasmas, Cascais, Portugal, June 22-July 3, 1998. *Physics of Space Plasmas, SPI Conference Proceedings and Reprint Series, Number 15*. T. Chang and J.R. Jasperse, eds. Cambridge: MIT Center for Theoretical Geo/Cosmo Plasma Physics, 1998, pp. 271-276.
- Ram, A.K., and A. Bers. "Heating or Cooling of Ions by Two Lower Hybrid Waves." *Proceedings of the International Sherwood Fusion Theory Conference*, Atlanta, Georgia, March 23-25, 1998, p. 1B03.
- Ram, A.K., A. Bers, and D. Bénisti. "Interaction of Ions With a Spectrum of Electrostatic Waves." *Proceedings of the Second Europhysics Topical Conference on RF Heating and Current Drive of Fusion Devices*, Brussels, Belgium, January 20-23, 1998. J. Jacquinot, G. Van Oost, and R.R. Weynants, eds. Petit-Lancy, Switzerland: European Physical Society, 1998, Contributed Papers, Vol. 22A, pp. 185-88.
- Ram, A.K., A. Bers, and D. Bénisti. "Ionospheric Ion Energization by Nonlinear Wave-Particle Interactions." *Eos (1998 American Geophysical Union Spring Meeting supplement)* 79: S314 (1998), paper SM41B-11.
- Ram, A.K., A. Bers, and L. Kang. "Nonlinear Energization and De-Energization of Ions by Two Lower Hybrid Waves." *Bull. Am. Phys. Soc.* 43: 1872 (1998).
- Ram, A.K., L. Kang, and A. Bers. "Nonlinear Ionospheric Ion Energization by Electrostatic Waves." *Eos (1998 American Geophysical Union Fall Meeting supplement)* 79: F769 (1998), paper SM31A-16.
- Schultz, S.D., A. Bers, and A.K. Ram. "Mode Conversion and Coupling to Electron Bernstein Waves in NSTX." *Proceedings of the International Sherwood Fusion Theory Conference*, Atlanta, Georgia, March 23-25, 1998, p. 2C15.
- Schultz, S.D., A.K. Ram, and A. Bers. "Mode-Converted Electron Bernstein Waves for Heating and Current Drive in NSTX." *Proceedings of the 17th International Atomic Energy Agency Fusion Energy Conference*, Yokohama, Japan, October 19-24, 1998. Vienna, Austria: IAEA. Paper IAEA-F1-CN-69/CDP/13. Forthcoming.

### Technical Reports

- Bénisti, D., A.K. Ram, and A. Bers. "Ion Dynamics in Multiple Electrostatic Waves in a Magnetized Plasma - Part I: Coherent Acceleration." Report No. PSFC/JA-98-4. Cambridge: MIT Plasma Science and Fusion Center, March 1998.
- Bénisti, D., A.K. Ram, and A. Bers. "Ion Dynamics in Multiple Electrostatic Waves in a Magnetized Plasma - Part II: Enhancement of the Acceleration." Report No. PSFC/JA-98-5. Cambridge: MIT Plasma Science and Fusion Center, March 1998.
- Bénisti, D., A.K. Ram, and A. Bers. "New Mechanisms of Ion Energization by Multiple Electrostatic Waves in a Magnetized Plasma." Report No. PSFC/JA-98-3. Cambridge: MIT Plasma Science and Fusion Center, March 1998.
- Bers, A., A.K. Ram, and S.D. Schultz. "Coupling to Electron Bernstein Waves in Tokamaks." Report No. PSFC/JA-98-6. Cambridge: MIT Plasma Science and Fusion Center, March 1998.
- Ram, A.K., A. Bers, and D. Bénisti. "Interaction of Ions with a Spectrum of Electrostatic Waves." Report No. PSFC/JA-98-7. Cambridge: MIT Plasma Science and Fusion Center, March 1998.

## 1.2 Physics of Thermonuclear Plasmas

### Sponsor

U.S. Department of Energy  
Grant DE-FG02-91ER-54109

### Project Staff

Professor Bruno Coppi, Dr. Augusta Airoidi, Ronak J. Bhatt, Dr. Giuseppe Bertin, Dr. Francesca Bombarda, Franco Carpignano, Dr. Giovanna Cenacchi, Dr. Riccardo Maggiore, Dr. Stefano Migliuolo, Dr. Francesco Pegoraro, Gregory Penn, Dr. Marco Riccitelli, Alexander Seidel, Dr. Linda E. Sugiyama, George M. Svolos

The activities of our group have covered a wide spectrum of plasma physics areas, from the physics of fusion burning plasmas, in which we have had a pioneering role and maintain a leading position, to plasma astrophysics and space physics (e.g., the partially ionized plasmas of the ionosphere). We have dealt with problems of basic theoretical plasma physics both by analytical and computational methods and have led the effort for the proposal and design of experiments to study ignition conditions in magnetically confined plasmas. Our work has received special recognition within the international scientific community, reflected, for instance, by a remarkable number of invited papers and by the success of the International Workshop on Ignitor that was recently held in Washington D.C.